Macromolecular Chemistry and Physics
www.mcp-journal.de

Fabrication of Thermally Crosslinked Hydrolyzed Polymers of Intrinsic Microporosity (HPIM)/Polybenzoxazine Electrospun Nanofibrous Membranes

Bekir Satilmis and Tamer Uyar**

In this study, thermally crosslinked hydrolyzed polymers of intrinsic microporosity (HPIM)/polybenzoxazine electrospun nanofibrous membranes (NFMs) are successfully produced. The nanofibers having 800 ± 260 to 670 ± 150 nm average fiber diameters from HPIM and blends of HPIM/benzoxazine (BA-a) ranging from HPIM:(BA-a) weight ratio of 9:1 to 2:1 *w*/*w* are produced by electrospinning. Self-standing HPIM/(BA-a) NFMs are thermally step-wise cured resulting in crosslinked HPIM/Poly(BA-a) NFMs. Structural characterization of as-electrospun HPIM/(BA-a) and crosslinked HPIM/Poly(BA-a) NFM is conducted by FT-IR spectroscopy to trace the ring opening and crosslinking reactions. Elemental analysis and XPS studies show an increase in carbon content and reduction in nitrogen content due to the crosslinking reaction. Decomposition temperature (T_d) of HPIM NFM increases from 218 to 270 °C with the crosslinking based on the DSC. DMA analysis shows that the mechanical strength of the NFMs has increased significantly with crosslinking. Young's moduli of HPIM NFM is increased from 16 ± 7 to 67 ± 1 MPa for crosslinked HPIM/Poly(BA-a)%33 NFM. Similarly, higher storage modulus is observed for HPIM/Poly(BA-a) NFMs compared to HPIM NFM. The crosslinked HPIM/Poly(BA-a) NFMs keep their fibrous morphology after solvent treatment in dimethylformamide revealing their structural stability compared to pristine HPIM NFM.

1. Introduction

Development of nanofibrous composite materials has attracted significant research interest in the recent years due to their unique properties such as high surface area and high porosity. Nanocomposite materials provide an opportunity to combine the properties of different materials to obtain improved mechanical, thermal, and chemical properties.[1,2] These materials with improved properties could be promising for numerous applications such as adsorption, separation, sensor, and catalysis applications. Electrospinning is a straightforward and cost-effective method to construct composite nanofibers from the variety of polymers and polymer blends.[3–5] Electrospun nanofibers have several attractive features including a high surface area to volume ratio and high porosity.[6] The electrospun nanofibers and their nanofibrous membranes (NFMs) hold great promise due to their outstanding properties when compared to bulk and film forms of the same materials.[7]

Polybenzoxazines are newly developing phenolic type resins, attracting considerable interest owing to their fascinating properties, such as high glass transition temperature, high char yield, and near-zero volumetric change upon curing.[8–11] These properties enable the production of high-performance composite materials.[12] Thus, immense research has been conducted on different forms of polybenzoxazines including bulk,[13,14] film,[15,16] aerogel,[17,18] membrane,[19] and nanofibers.[20,21] However, far too little attention has been paid to the incorporation of polybenzoxazine into polymeric nanofibers.[12,22]

Recently, a new type of polymer named polymers of intrinsic microporosity (PIMs) has been introduced and has gathered significant attention from various fields owing to their high surface area, high thermal, and chemical stabilities.[23–25] PIM-1 is the first polymer that is introduced from this family and it showed outstanding properties in adsorption and separation applications.[24,26] Thanks to its processability in common organic solvents, PIM-1 has been widely used in the form of powder and film.[27–29] Recently, fiber form has also started gathering momentum; for instance, fibers of PIM-1 can be prepared by electrospinning technique that opens up additional application areas to PIM-based polymeric materials.[30–33] PIM-1 has nitrile groups in the backbone that can be modified by simple hydrolysis to tailor the properties of polymer for desired applications.[34] Recently, we have reported electrospun-hydrolyzed PIM-1 (HPIM) NFM and its effective usage in methylene blue removal from an aqueous system since HPIM has an affinity

Dr. B. Satilmis, Prof. T. Uyar
National Nanotechnology Research Center
Institute of Materials Science and Nanotechnology (UNAM)
Bilkent University
Ankara 06800, Turkey
E-mail: bekir.satilmis@ahievran.edu.tr; tamer@unam.bilkent.edu.tr
Dr. B. Satilmis
Department of Chemistry
Faculty of Science and Arts
Ahi Evran University
Kirsehir 40100, Turkey
The ORCID identification number(s) for the author(s) of this article can be found under https://doi.org/10.1002/macp.201800326.

DOI: 10.1002/macp.201800326

toward cationic species.[35] Despite the outstanding adsorption performance of HPIM, there is still room for improvement of the mechanical and chemical stability of this membrane. Hence, attention has been paid to improve the mechanical and chemical stability of HPIM by incorporating hexamethylene diisocyanate into the membrane.[36] The resulting crosslinked membranes showed much higher mechanical and chemical stability while losing their thermal stability with respect to pristine HPIM fibrous membrane.[36]

In this study, we have aimed to improve the thermal and mechanical properties of electrospun HPIM nanofibers by crosslinking with benzoxazine (BA-a monomer). Despite the interest on both materials, to the best of our knowledge, there has been no study related to crosslinking HPIM with benzoxazines. Here, bead-free and uniform NFMs were obtained from different compositions of HPIM and BA-a blend solutions (9:1 to 2:1 *w*/*w*) by electrospinning. Following that, crosslinking was accomplished by thermal curing of HPIM/BA-a NFMs. The thermally crosslinked HPIM/Poly(BA-a) NFMs showed enhanced structural stability together with improved thermal and mechanical properties compared to pristine HPIM NFM.

2. Experimental Section

2.1. Materials

PIM-1 was synthesized according to the previous method[33] using 5,5′,6,6′-tetrahydroxy-3,3,3′,3′-tetramethyl-1,1′-spirobisindane (98%, Alfa Aesar) and tetrafluoroterephthalonitrile (98%, Aldrich) monomers in the presence of potassium carbonate.[33] Aniline (99%), bisphenol-A (97%), paraformaldehyde (95%), ethanol, sodium hydroxide (NaOH), and dimethylformamide (DMF) were purchased from Sigma-Aldrich and they were used without further purification.

2.2. Synthesis of Hydrolyzed PIM-1 (HPIM)

Hydrolysis of PIM-1 was achieved according to previously described method.[35] PIM-1 powder was mixed with NaOH solution (water/ethanol: 1/1, *v*/*v*) in a one-neck round bottom flask which was fitted with a condenser. Afterward, the mixture was heated up to 120 °C and left to stir at this temperature under reflux for 3 h. Once the reaction stopped, deionized water was poured into the reaction mixture and solid was collected by vacuum filtration. The product was dried in an oven at 110 °C overnight prior to being placed in acidic water (pH ≈ 4–5) and was stirred at room temperature for 2 h. Solid was collected by vacuum filtration and was placed in deionized water for 1 h. Following this, the final product was filtered and washed with a copious amount of water. The resulting HPIM powder was dried in an oven at 110 °C overnight.

2.3. Synthesis of Benzoxazine Monomer (BA-a)

Benzoxazine monomer (BA-a) was synthesized according to solventless method.[9] Bisphenol-A (0.05 mol), aniline (0.1 mol), and paraformaldehyde (0.2 mol) were placed in a 100 mL one-neck round bottom flask and were mixed at room temperature for a couple of minutes. Then the mixture was heated up to 110 °C in an oil bath and kept at this temperature for 1.5 h while it is stirring. BA-a monomer was obtained as a transparent, highly viscous liquid which was then cooled down before dissolving in chloroform. The product was extracted by 3 M NaOH solution (four times) and by water (three times). The organic phase was dried using sodium sulfate before evaporating the chloroform with the help of a rotary evaporator. The product was dried in a vacuum oven at 70 °C for 5 h while maintaining the desired pressure. A highly viscous liquid, was immediately solidified after removing from oven and was grinded by mortar and pestle. BA-a monomer was obtained in the form of a bright yellow powder.

2.4. Electrospinning of Nanofibers

The chemical structures of HPIM and BA-a, and the electrospinning process are illustrated in **Figure 1**. The homogenous solutions (0.5 mL) of HPIM and blends of HPIM/(BA-a) were prepared in DMF. The concentration of HPIM was kept constant at 50% *w*/*v* with respect to the solvent. HPIM/(BA-a) blends were prepared by mixing and dissolving HPIM powder and the predetermined amount of the BA-a monomer (10, 25, and 33% *w*/*w*, with respect to total weight) in DMF at room temperature for 3 h. The compositions of HPIM/(BA-a) blends are provided in **Table 1**. Each solution was placed in 1 mL plastic syringe which was fitted with the metallic needle (0.5 mm outer diameter) and it was placed horizontally on a syringe pump (KD Scientific, KDS 101). Electrospinning was achieved by applying the given parameters; 11.5 kV voltage, 0.5 ml h^{-1} flow rate and 15 cm distance. Electrospun nanofibers were collected randomly in the form of NFM on an aluminum foil. Afterward, the electrospun NFMs were dried in a fume hood overnight. The samples were marked as as-electrospun HPIM and HPIM/(BA-a)%10-33 NFMs.

2.5. Curing Studies of Electrospun Nanofibrous Membranes

Crosslinking was achieved using thermal crosslinking strategy between HPIM and (BA-a) monomer. The electrospun nanofibers of HPIM/(BA-a) blends were subjected to step-wise thermal treatment in an oven from 150 to 225 °C (150, 175, 200, and 225 °C for an hour for each temperature) to initiate ring opening of (BA-a) and crosslinking of the HPIM/(BA-a) nanofibrous matrix. The samples were coded as "thermally treated HPIM NFM, and crosslinked HPIM/Poly(BA-a)%10-33" after the completion of crosslinking.

2.6. Measurements and Characterization

Bruker DPX-400 MHz spectrometer was used to record ^{1}H-NMR spectra of samples at room temperature. Peak integrations were calculated using Spinwork 3 software. Fourier transform infrared (FT-IR) spectrometer (Bruker Vertex 70) was

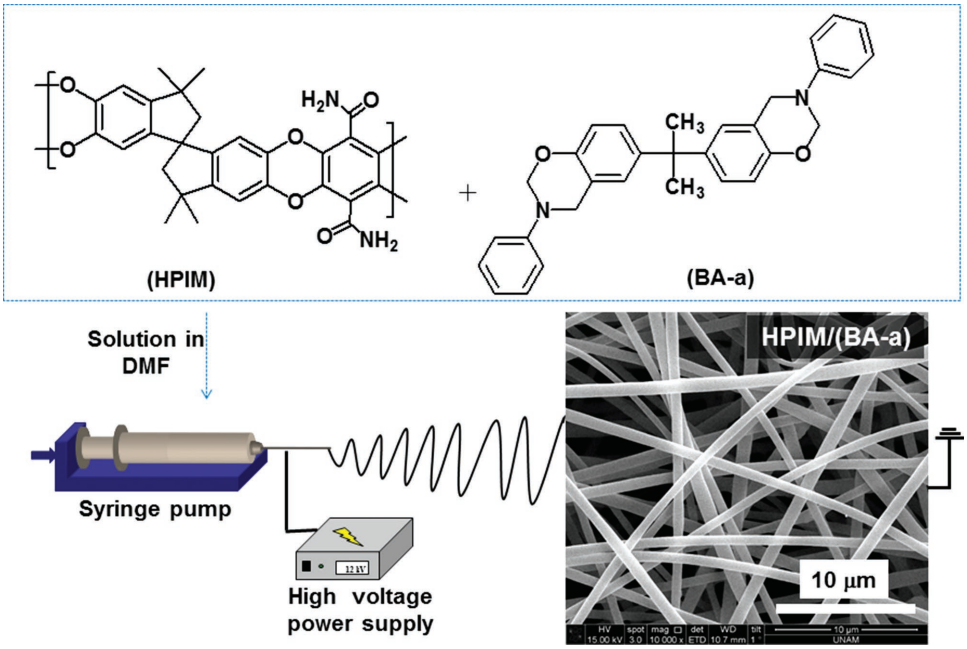

Figure 1. Chemical structures of HPIM and BA-a and schematic representation of electrospinning of nanofibers from HPIM/(BA-a) blend.

used to monitor the functional groups in NFMs. Peak areas were determined using Omnic software. The morphology of the nanofibers was monitored by scanning electron microscopy (FEI Quanta 200 FEG). Fiber diameters together with the fiber distribution were determined using ImageJ software by measuring about 100 different fibers. The elemental compositions of the NFMs were assessed by elemental analysis (Thermo Scientific Flash 2000 series CHNS-O analyzer). The elemental surface composition of the NFMs were identified by X-ray Photo electron spectroscopy (XPS, Thermo Scientific), equipped with a monochromatic Al/Ka as the X-ray source and the data was analyzed with Advantage software. Thermal analyses of the NFMs were conducted with a TGA (TA Q500) and DSC (TAQ2000) under nitrogen atmosphere. The applied heating rate was 20 °C min^{-1} for both techniques. Mechanical properties of the NFMs were tested using dynamic mechanical analyzer (DMA, Q800 TA Instruments). Rectangular-shaped specimens (8 × 6 × 0.1 mm) were tested to obtain stress–strain curves in controlled force mode with 0.05 N min^{-1} force ramp rate for two different samples at room temperature. Young's moduli of the samples were calculated from the linear region of the curves. Additionally, storage moduli were recorded in multifrequency mode with an amplitude value of 5 µm for the same size of samples. Samples were heated up to 300 °C at 3 °C min^{-1}. The water contact angle (WCA) of the NFMs were measured by a contact angle goniometer (OCA20, Dataphysics, Germany). The thin NFMs (2 × 3 cm^2) were placed on a glass slide. A drop of distilled water (4 µL) was dropped onto the membrane automatically and Laplace–Young fitting was applied on measurements. Tests were repeated five times, and the data was expressed as mean ± SD. Both as-electrospun and crosslinked NFMs were kept in electrospinning solvent (DMF) overnight to investigate the structural stability of crosslinked membranes. Then, materials were removed from DMF and were dried at room temperature before SEM imaging. Similarly, the success of crosslinking was monitored using the same approach by deuterated DMSO. Both

Table 1. Sample codes, content of the samples, experimental, and theoretical % elements based on elemental analysis and XPS.

Sample code	Content		Elemental analysis						XPS [%]		
			Experimental [%]			Theoretical [%]					
	HPIM	BA-a	N	C	H	N	C	H	N	C	O
HPIM Powder	100	0	4.9	63.1	5.2	–	–	–	–	–	–
BA-a Powder	0	100	5.9	77.2	6.3	–	–	–	–	–	–
HPIM NFM (thermally treated)	1	0	5.0	65.1	5.1	4.9	63.1	5.2	5.3	78.6	16.1
HPIM/Poly(BA-a)%10 NFM	0.9	0.1	4.8	66.1	5.0	5.0	64.5	5.3	4.7	79.2	16.2
HPIM/Poly(BA-a)%25 NFM	0.75	0.25	4.5	67.8	4.8	5.2	66.7	5.4	3.9	80.4	15.8
HPIM/Poly(BA-a)%33 NFM	0.67	0.33	4.4	68.6	5.0	5.2	67.8	5.5	3.8	80.3	15.9

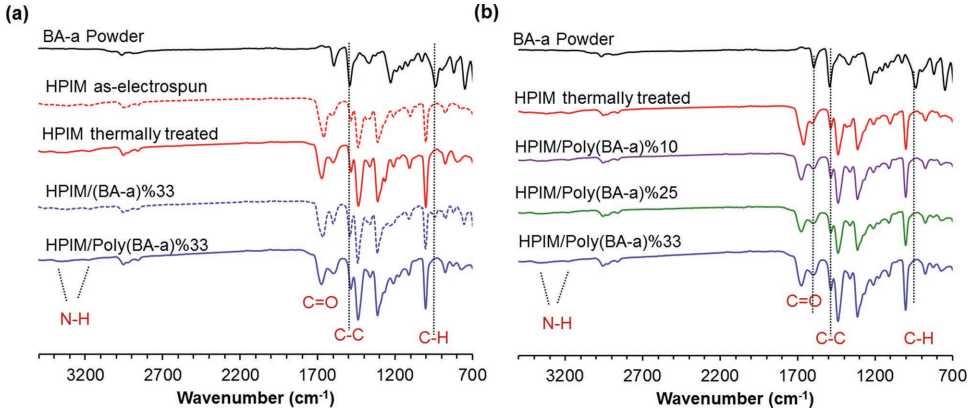

Figure 2. FT-IR spectra of a) BA-a powder, as-electrospun and thermally treated HPIM NFM, as-electrospun HPIM/(BA-a)%33 NFM and crosslinked HPIM/Poly(BA-a)%33 NFM; b) BA-a powder, thermally treated HPIM NFM, and crosslinked HPIM/Poly(BA-a) NFMs.

blend and crosslinked fibrous membranes were kept in deuterated DMSO (used as NMR solvent), then the insoluble part was removed from the solution with the help of a tweezer and the remaining solution was measured by ^{1}H-NMR and compares with each other.

3. Results and Discussion

3.1. Structural Characterization of HPIM and BA-a

Structural characterization of parent PIM-1 polymer was performed in our previous studies.[33,35] ^{1}H-NMR and FT-IR spectra, and TGA curve of PIM-1 are provided in Figures S1–S3, Supporting Information. PIM-1 was fully hydrolyzed in the presence of NaOH until the complete conversion of nitrile to amide as reported previously.[34] In addition, BA-a monomer was synthesized by the solventless method using bisphenol-A, aniline, and paraformaldehyde.[9] The purity and structure of HPIM and BA-a were confirmed by ^{1}H-NMR and FT-IR spectroscopies. The characterization of HPIM and BA-a are now well established. Figure S1, Supporting Information shows ^{1}H-NMR spectra of HPIM and BA-a. The amide protons of HPIM are located between 7 and 8 ppm (H5), aromatic peaks appear at 6–7 ppm (H3 and H4). In addition, aliphatic peaks appear below 2 ppm (H1 and H2). Furthermore, the peak intensity ratio of aliphatic to aromatic protons is 4:1 which confirms the successful modification of PIM-1 to hydrolyzed PIM-1.[36] The characteristic benzoxazine signals are also displayed in Figure S1, Supporting Information, which shows four different proton environments. Multiple aromatic protons are observed between 6 to 8 ppm. Oxazine ring formation was confirmed by the peaks at 5.3 and 4.6 which are associated with O-CH2-N (Ha) and Ph-CH2-N (Hb), respectively. The peak intensity ratio of these peaks is 1:1 that reveals the high purity of BA-a.[22] **Figure 2**a illustrates the FT-IR spectra of HPIM and BA-a. After the hydrolysis, characteristic nitrile stretches (2240 cm^{-1}) of PIM-1 completely disappeared while the peaks between 3500 and 3000 cm^{-1} (NH) appeared together with carbonyl peaks associated with amide 1 and amide 2 at 1680 and 1590 cm^{-1}. Furthermore, the characteristic peaks of the benzoxazine structure are also presented in Figure 2a. The peak at 1490 cm^{-1} shows C–C stretching of BA-a and C–H stretches can be seen at 940 cm^{-1}. Additionally, the peak at 1232 cm^{-1} is associated with asymmetric stretches of C—O—C in the oxazine ring.

3.2. Electrospinning of Nanofibrous Membranes

Electrospinning of HPIM was performed based on our previous study.[35] Homogenous solutions of the HPIM and blend solutions of HPIM/(BA-a) were prepared in DMF. The lowest concentration of HPIM to obtain bead-free and uniform fiber morphology was determined to be 50% *w*/*v*. Electrospun nanofibers with different compositions were produced using different ratios of HPIM/(BA-a) solutions in DMF. The samples were coded as "as-electrospun HPIM/(BA-a)%x NFM" in which *x* represents the relative ratio of BA-a monomer with respect to total weight and NFM for nanofibrous membrane. Detailed data for the composition of the samples are provided in Table 1. **Figure 3** illustrates SEM images and fiber diameter distributions of as-electrospun HPIM and HPIM/(BA-a) NFMs. All samples display rounded, bead-free, and uniform fiber morphology as confirmed by SEM imaging. The average fiber diameter (AFD) of pristine HPIM NFM was measured as 800 ± 260 nm. After the addition of BA-a to the polymer solution, no significant change was observed in AFD of HPIM/(BA-a) NFMs, yet, slightly narrower fiber distributions were obtained with the addition of BA-a as shown in Figure 3.

Following the successful production of self-standing NFMs, curing studies were conducted in the certain temperature range to initiate the crosslinking without giving any damage on HPIM structure. The crosslinking of the HPIM/(BA-a) NFMs was performed by thermal curing. Crosslinked NFMs were obtained and they were expressed as "crosslinked HPIM/Poly(BA-a)." As reported by Ning and Ishida,[9] step-wise thermal curing from 150 to 225 °C (samples were kept at 150, 175, 200, and 225 °C for an hour for each temperature) was performed on blends of HPIM/(BA-a) NFMs to start ring opening of BA-a monomer and crosslinking reaction between HPIM and BA-a. As-electrospun HPIM NFM was also subjected to the same thermal treatment as a control experiment to investigate the

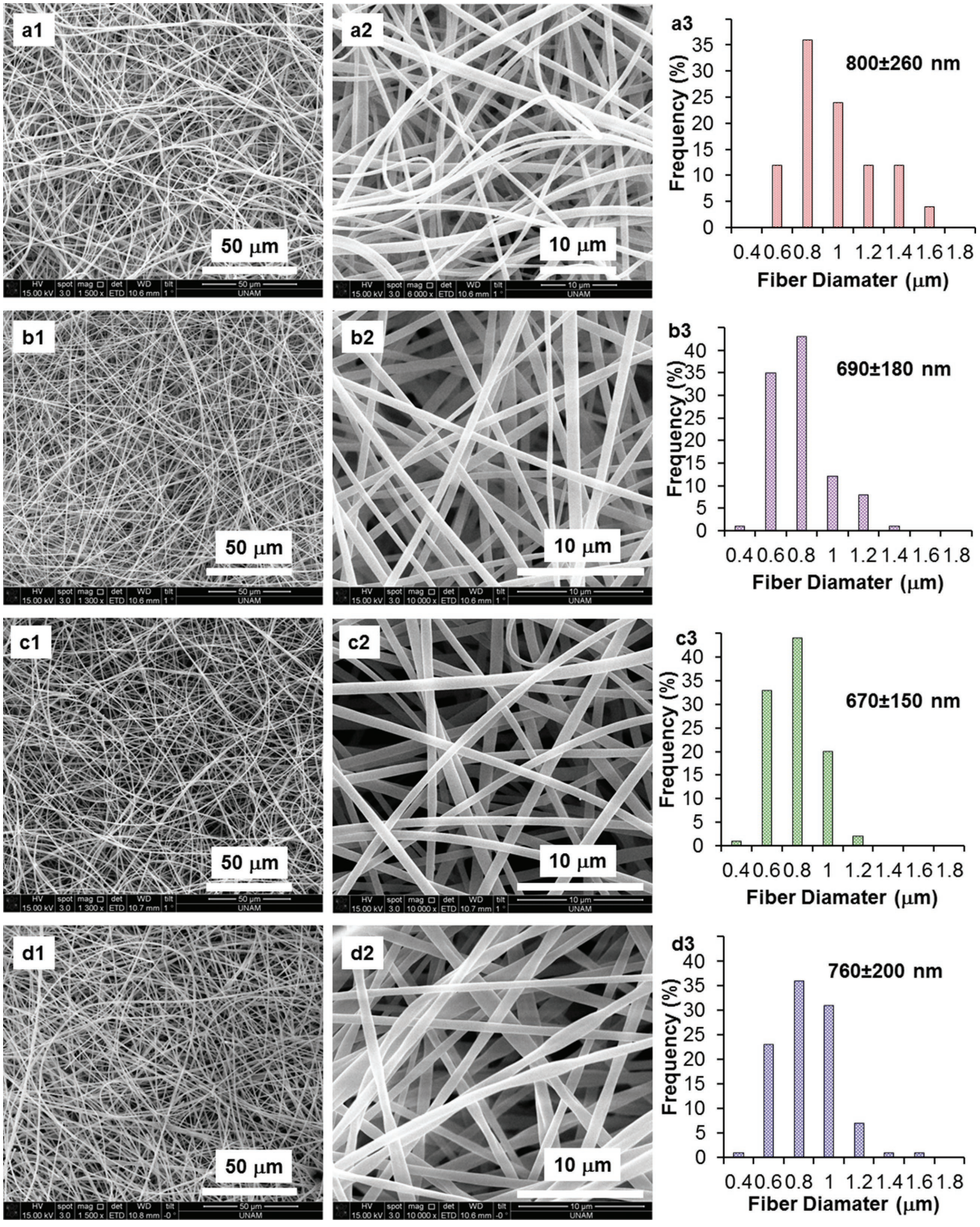

Figure 3. SEM images and fiber diameter distributions of as-electrospun a) HPIM NFM, b) HPIM/(BA-a)%10, c) HPIM/(BA-a)%25, and d) HPIM/(BA-a)%33 NFMs. 1) At lower magnification images, 2) higher magnification images, 3) fiber diameter distributions and AFD values of corresponding samples.

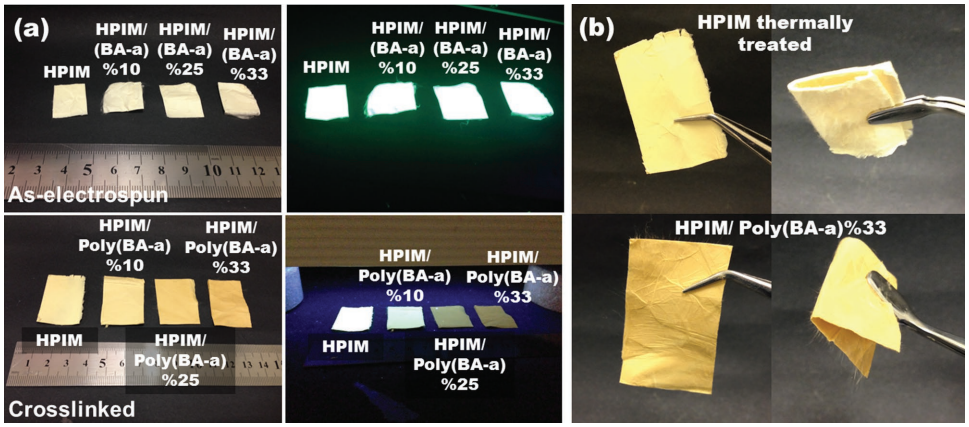

Figure 4. Digital images of a) as-electrospun (top) and crosslinked (bottom) nanofibrous membranes under day light (left) and UV light (right). b) Flexibility of thermally treated HPIM NFM and crosslinked HPIM/Poly(BA-a)%33 NFM.

effect of thermal treatment on HPIM structure. Two possible crosslinkings may occur in NFMs; first one is in-between BA-a monomers and the second one is in-between BA-monomer and amide functionality of HPIM. Possible anticipated structure of crosslinked HPIM/Poly(BA-a) is provided in Figure S4, Supporting Information. The effect of thermal treatment on NFMs can be monitored visually by naked eye. While pristine HPIM NFM and HPIM/(BA-a) NFMs are in white-off color, the crosslinked HPIM/Poly(BA-a) NFMs have changed their color to light/dark brown. Visual differences between NFMs before and after curing are displayed in **Figure 4**a. After thermal treatment, pristine HPIM NFM shows light brown color which is actually the color of the powder form. On the other hand, the intensity of the brown color has increased in correlation with the increasing amount of BA-a in the HPIM/Poly(BA-a) NFMs after curing. Furthermore, HPIM has fluorescence characteristic; hence, pristine HPIM NFM and HPIM/(BA-a) NFMs were monitored under UV light and all samples clearly showed fluorescence before crosslinking. However, the fluorescence was diminished for crosslinked HPIM/Poly(BA-a) NFMs after curing which indicated the success of crosslinking between HPIM and BA-a (Figure 4a).

SEM analysis of the membranes after crosslinking revealed that the fibrous structure of all membranes was maintained. Additionally, the fiber diameter distributions of all membranes remained almost the same after thermal treatment as exhibited in **Figure 5**. The structural characterizations of the as-electrospun and crosslinked membranes were analyzed using FT-IR spectroscopy. Figure 2a displays the as-electrospun and thermally treated HPIM NFM and as-electrospun HPIM/(BA-a)%33 NFM and crosslinked HPIM/Poly(BA-a)%33 NFM. No significant change is observed in HPIM NFM after thermal treatment. FT-IR and ^{1}H-NMR spectra and TGA curves of HPIM NFMs at different thermal treatment temperatures are provided in Figures S2a,b and S3, Supporting Information. The chemical stability of amide groups of HPIM was first confirmed by FT-IR spectroscopy using the intensity ratios of C-H (3010–2820 cm^{-1}) to N-H (3540–3020 cm^{-1}) which are presented in Table S1, Supporting Information. The ratio of I_{CH}/I_{NH} remained ≈0.44 within an experimental error. Further support for the stability of amide groups of HPIM was provided by ^{1}H-NMR spectroscopy using the integration of amide protons (H5) to aromatic protons of HPIM (H3) which also showed negligible difference after thermal curing (Table S1, Supporting Information). Also, the thermal degradation of as-electrospun and thermally treated HPIM NFMs are almost identical within an experimental error. Moreover, the difference between as-electrospun HPIM/(BA-a)%33 NFM and crosslinked HPIM/Poly(BA-a)%33 NFM can be monitored easily. As-electrospun HPIM/(BA-a)%33 NFM shows characteristic benzoxazine stretches at 1490 and 940 cm^{-1} that should reduce the intensity after crosslinking due to the structural change in benzoxazine ring.[22] As expected, while the intensity of the peak at 1490 cm^{-1} is reduced, the intensity of the peak at 940 cm^{-1} disappeared after curing. Figure 2b illustrates the FT-IR spectra of BA-a monomer, thermally treated HPIM, and all crosslinked HPIM/Poly(BA-a) NFMs after thermal crosslinking. As can be seen, the peak at 940 cm^{-1} is invisible in all samples, indicating successful crosslinking of the HPIM/Poly(BA-a) NFMs.

Following infrared spectroscopy, elemental compositions were determined using elemental analysis to investigate the structural changes in HPIM/Poly(BA-a) NFMs after crosslinking, depending on the amount of BA-a in the membrane. Table 1 illustrates the elemental compositions of HPIM and BA-a powders in which both possess significant carbon content along with nitrogen content. The amount of nitrogen and carbon in BA-a monomer is slightly higher than that of HPIM, suggesting an increase in the amount of nitrogen and carbon in blend (HPIM/BA-a) membranes. In addition, thermally treated HPIM NFM does not show any significant change after thermal treatment. Hence, by taking powder data as a theoretical value, the theoretical compositions of the crosslinked HPIM/Poly(BA-a) NFMs samples were calculated, as expressed in Table 1. Experimental elemental analysis of crosslinked HPIM/Poly(BA-a) NFMs showed that (Table 1) while the relative intensity of carbon is increasing, the relative intensity of nitrogen is reduced after curing. Therefore, theoretical versus experimental carbon and nitrogen contents were investigated and they showed a similar trend in an opposite way as illustrated in Figure S5a-b, Supporting Information in which it is suggested that the crosslinking may occur between BA-a and HPIM amide group. As shown, HPIM structure is

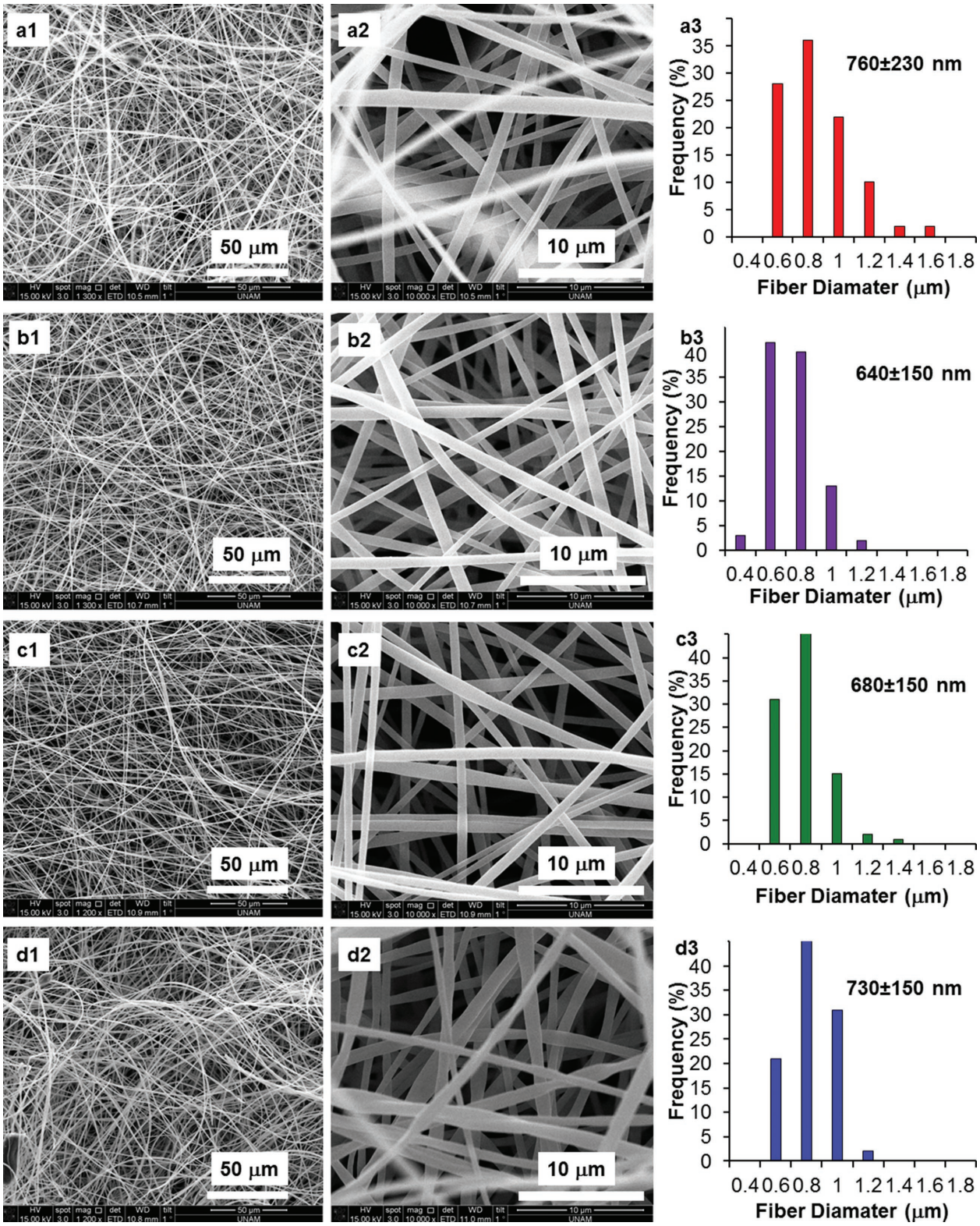

Figure 5. SEM images and fiber diameter distributions of a) thermally treated HPIM NFM, and crosslinked b) HPIM/Poly(BA-a)%10, c) HPIM/Poly(BA-a)%25, and d) HPIM/Poly(BA-a)%33 NFMs. 1) At lower magnification, 2) at higher magnification, 3) and fiber diameter distributions and the AFD of the corresponding samples.

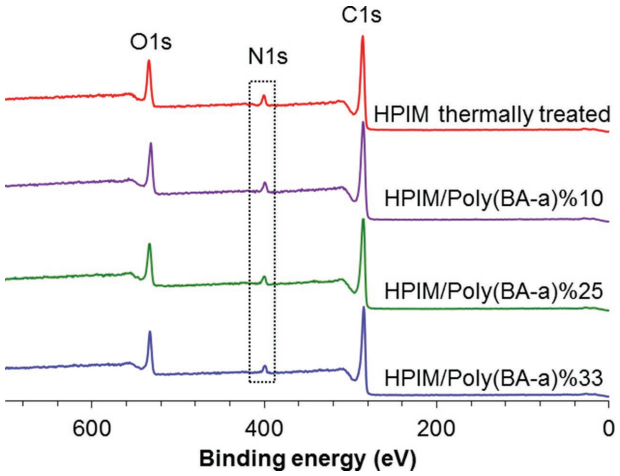

Figure 6. XPS spectra of thermally treated HPIM NFM and crosslinked HPIM/Poly(BA-a) NFMs.

stable without using BA-a monomer. A possible explanation for the reduction in nitrogen content is that when benzoxazine ring is opened in thermal treatment it may react with the carbonyl group in HPIM. Following this, amide functionality would lose as the temperature (225 °C) is close to amide degradation temperature (250 °C). This was supported later by thermal analysis study. The study further continued with the surface analyses of the NFM samples by using XPS technique.

Figure 6 illustrates the XPS spectra of thermally treated HPIM NFM and crosslinked HPIM/Poly(BA-a) NFMs. As can be seen, all samples show carbon (285 eV), nitrogen (399 eV), and oxygen peaks (533 eV). The intensity of oxygen is almost the same in all samples (Table 1). However, the intensity of carbon slightly increased while the intensity of nitrogen reduced slightly which is in accordance with elemental analysis (Table 1 and Figure 6). Moreover, a good agreement in the relative ratio of N/C obtained by elemental analysis versus XPS can be seen in Figure S5c, Supporting Information.

After structural analyses, thermal properties of NFM were investigated using TGA and DSC techniques. **Figure 7**a shows TGA curves of thermally treated HPIM and crosslinked HPIM/Poly(BA-a) NFMs. Pristine HPIM is stable up to 250 °C; thus, no significant improvement was expected with benzoxazine crosslinking and it is difficult to observe significant improvement in TGA. However, DSC gives more information about the crosslinked samples. As shown in Figure 7b, BA-a monomer displays exothermic peak which is characteristic for this material. After curing, this peak should reduce or disappear. PIM polymers are thermally stable that no T_g can be observed before the polymer degradation.[37] As-electrospun and thermally treated HPIM NFM shows no difference in DSC, they both give two endothermic peaks at 158 and 218 °C. The first one is possibly relaxation of the polymer chains as we investigated in detail in our previous study[35] and that was not a T_g. The second one (218 °C, T_d) is the degradation of the polymer. In addition, as-electrospun HPIM/(BA-a)%33 NFM shows two

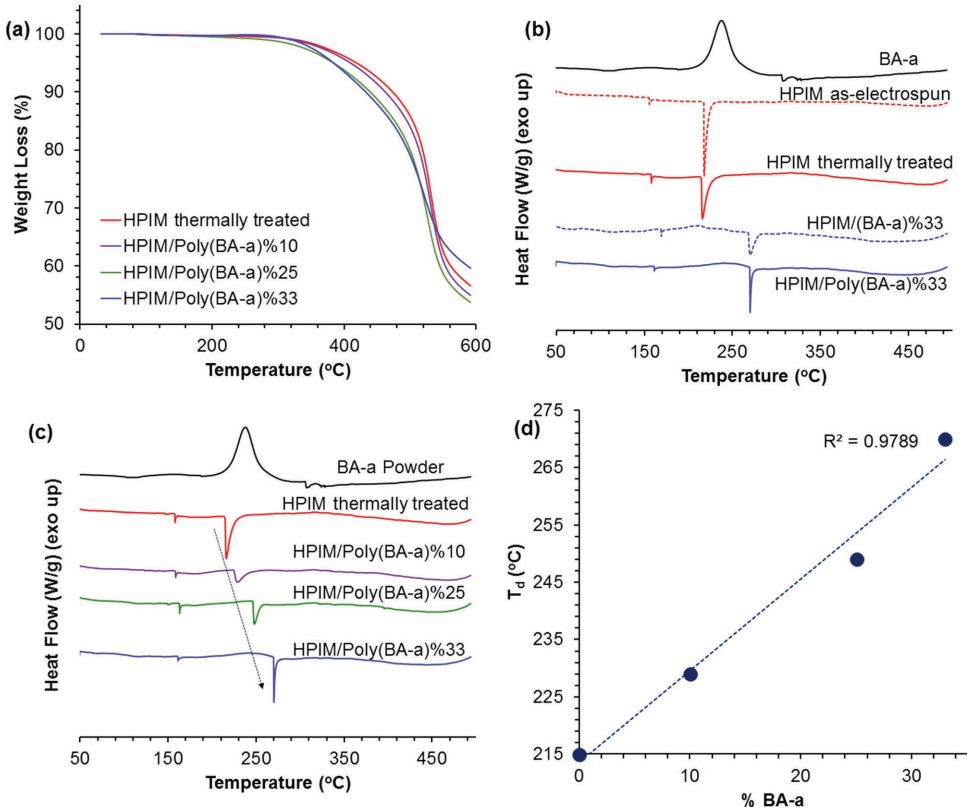

Figure 7. a) TGA thermogram, b–c) DSC curves of NFM samples, and d) the relationship between T_d versus BA-a content of NFMs.

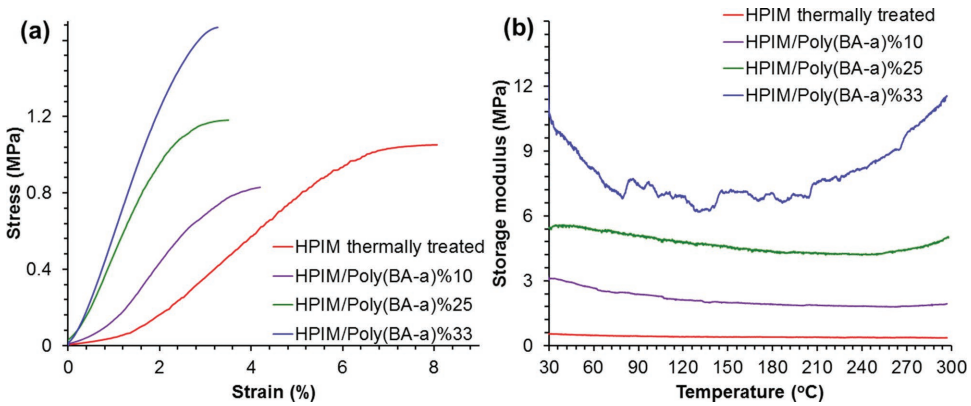

Figure 8. a) Stress–strain curves of b) storage modulus of thermally treated HPIM NFM and crosslinked HPIM/Poly(BA-a) NFMs.

endothermic peaks at 160 and 270 °C. Also, an exothermic peak appeared at 220 °C due to the BA-a. After curing, this peak disappeared while the other two remained the same (Figure 7b). Polymer degradation temperature, T_d, was increased by more than 50 °C. Moreover, the increase in T_d has a direct correlation with the amount of BA-a in the membrane (Figure 7c). A good correlation between T_d versus BA-a content of the membranes is presented in Figure 7d.

Figure 4b exhibits that both thermally treated HPIM NFM and HPIM/Poly(BA-a)%33 NFM are self-standing and flexible materials that can be quite useful for certain applications. Mechanical properties of NFMs were also improved with crosslinking. All mechanical tests were conducted at least two times to increase the reliability of the measurements. **Figure 8**a displays representative stress–strain curves of the samples. Young's moduli of the samples were calculated from the linear region of these curves. As the beginning stress causes an alignment in HPIM NFM and HPIM/Poly(BA-a)%10 NFM, we have applied this way of calculation. Hence, Young's moduli of the HPIM increased from 16 ± 7 to 67 ± 1 MPa with the crosslinking. A good correlation between Young's modulus and BA-a content of the membranes can be seen in Figure S6, Supporting Information. In addition, storage modulus of the samples is displayed in Figure 8c indicating a significant improvement in mechanical behavior of the membranes.

Moreover, WCA measurements were conducted to investigate the effect of crosslinking on the hydrophobicity of HPIM NFM. The WCA and the digital images how water droplet remains on the NFM surface are provided in **Figure 9**. As reported,[36] electrospun HPIM NFM is a hydrophobic membrane having WCA of ≈140° due to the surface roughness. After crosslinked with benzoxazine, almost same WCA ≈140°) was observed for crosslinked HPIM/Poly(BA-a)%33 NFM (Figure 9) indicating that the HPIM/Poly(BA-a) NFM has also hydrophobic character which may be useful in water treatment applications as filtering materials.

Along with thermal and mechanical improvement, structural stability of the membranes and the success of crosslinking was investigated using good solvents (DMF) which was used for electrospinning. While all as-electrospun NFM samples are immediately dissolved in DMF, crosslinked HPIM/Poly(BA-a) NFMs show an improved resistance in correlation with the amount of BA-a content in the membrane (Figure S7,

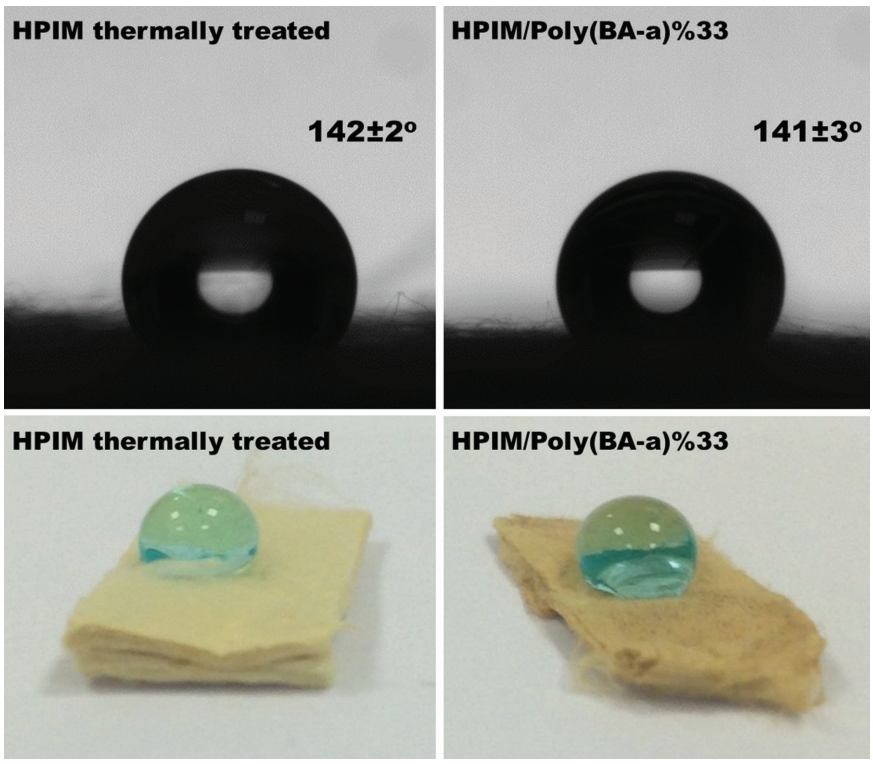

Figure 9. (Top) Water contact angle images of and (bottom) water droplets on a piece of thermally treated HPIM and crosslinked HPIM/Poly(BA-a)%33 NFMs. Water was colored with methylene blue dye for a better contrast.

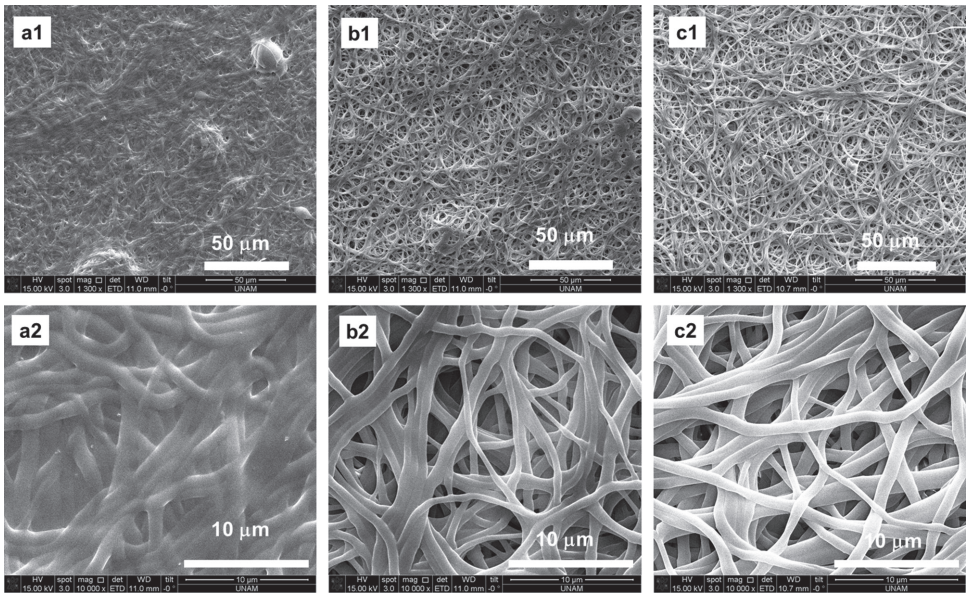

Figure 10. SEM images of crosslinked a) HPIM/Poly(BA-a)%10, b) HPIM/Poly(BA-a)%25, and c) HPIM/Poly(BA-a)%33 NFMs after DMF treatment. 1) At lower magnification images, 2) at higher magnification images.

Supporting Information). HPIM NFM was still soluble after thermal treatment; nevertheless, crosslinked HPIM/Poly(BA-a) NFMs showed enhanced stability against DMF treatment. SEM images of crosslinked HPIM/Poly(BA-a) NFMs after DMF treatment are displayed in **Figure 10**. While HPIM/Poly(BA-a)%10 NFM has shown more swelling and some film forming structure on the surface, HPIM/Poly(BA-a)%33 NFM has shown the most stable structure keeping its fibrous morphology due to more crosslinking in HPIM/Poly(BA-a)%33 NFM. Subsequently, another good solvent (DMSO) was employed to determine the success of crosslinking and unreacted monomers in fibrous membranes after thermal treatment. Both HPIM/(BA-a) and HPIM/Poly(BA-a) NFMs were placed in deuterated DMSO and solutions were characterized by ^{1}H-NMR spectroscopy. As can be seen in Figure S8, Supporting Information, while HPIM/ (BA-a) NFMs are readily soluble in DMSO, HPIM/Poly(BA-a) NFMs do not show any discernible peaks in ^{1}H-NMR spectrum, even in 50 times magnified NMR spectrum, no significant peaks were determined, showing that no detectable unreacted monomer remains in fibrous membranes.

4. Conclusions

In this study, crosslinked HPIM/Poly(BA-a) electrospun NFMs were produced having enhanced thermal, mechanical, and structural properties depending on the amount of benzoxazine present in HPIM matrix. First, self-standing HPIM/(BA-a) NFMs having bead-free and uniform fiber morphology were obtained via electrospinning, then, crosslinking was achieved using only curing method without the necessity of crosslinking agent. Crosslinking between HPIM and BA-a in HPIM/(BA-a) NFMs was investigated using FT-IR spectroscopy by tracing the ring opening of benzoxazine resin. In addition, elemental analysis and XPS techniques were performed to determine the reduction in nitrogen content as an evidence for chemical interaction between HPIM and BA-a. While crosslinking has no adverse effect on fiber morphology as confirmed by SEM analysis, the thermal resistance of NFMs increased by almost 50 °C based on DSC results. The tensile stress–strain measurements revealed that crosslinked HPIM/Poly(BA-a)%33 NFM exhibited a higher strength with a Young's modulus of 67 ± 1 MPa which was higher than that of pristine HPIM NFM (16 ± 7 MPa). In addition, crosslinking between HPIM and BA-a in HPIM/Poly(BA-a) NFM was further proved by the solubility test. While all as-electrospun HPIM/(BA-a) NFM samples are readily soluble in a good solvent (i.e., DMF), crosslinked HPIM/Poly(BA-a) NFMs showed enhanced solvent resistance by maintaining their fibrous structure. As expected, crosslinking of HPIM with benzoxazine provided an opportunity to combine the properties of these two high-performance materials. This research has tended to focus on improving the properties of HPIM fibrous membranes with the thermal crosslinking rather than investigating crosslinking mechanism. Thus, we have avoided overpredicting the structure as the materials are not completely soluble. We believe that the current findings so far have been promising and may help to trigger the growing body of literature on PIM-polybenzoxazine composites materials, as this is the first related report in the literature to the best of our knowledge.

Supporting Information

Supporting Information is available from the Wiley Online Library or from the author.

Conflict of Interest

The authors declare no conflict of interest.

Keywords

electrospinning, membranes, nanofibers, polybenzoxazine, polymers of intrinsic microporosity

Received: July 30, 2018
Revised: August 29, 2018
Published online: September 21, 2018

[1] L. Zhang, T. J. Webster, *Nano Today* **2009**, *4*, 66.
[2] R. Sahay, P. S. Kumar, R. Sridhar, J. Sundaramurthy, J. Venugopal, S. G. Mhaisalkar, S. Ramakrishna, *J. Mater. Chem.* **2012**, *22*, 12953.
[3] S. Ramakrishna, K. Fujihara, W.-E. Teo, T.-C. Lim, Z. Ma, *An Introduction to Electrospinning and Nanofibers*, World Scientific, Singapore **2005**.
[4] T. Uyar, E. Kny, *Electrospun Materials for Tissue Engineering and Biomedical Applications: Research, Design and Commercialization*, Elsevier, Woodhead Publishing, Cambridge, UK **2017**.
[5] A. Senthamizhan, A. Celebioglu, S. Bayir, M. Gorur, E. Doganci, F. Yilmaz, T. Uyar, *ACS Appl. Mater. Interfaces* **2015**, *7*, 21038.
[6] A. Celebioglu, T. Uyar, *Mater. Lett.* **2011**, *65*, 2291.
[7] J. H. Wendorff, S. Agarwal, A. Greiner, *Electrospinning: Materials, Processing, and Applications*, John Wiley & Sons, Weinheim, Germany **2012**.
[8] N. N. Ghosh, B. Kiskan, Y. Yagci, *Prog. Polym. Sci.* **2007**, *32*, 1344.
[9] X. Ning, H. Ishida, *J. Polym. Sci., Part A: Polym. Chem.* **1994**, *32*, 1121.
[10] H. Ishida, D. J. Allen, *J. Polym. Sci., Part B: Polym. Phys.* **1996**, *34*, 1019.
[11] J. Hacaloğlu, T. Uyar, H. Ishida, *Handbook of Benzoxazine Resins* (Eds: H. Ishida,T. Agag), Elsevier, Amsterdam **2011**, p. 287.
[12] Y. Ertas, T. Uyar, *Advanced and Emerging Polybenzoxazine Science and Technology* (Eds: H. Ishida,P. Froimowicz), Elsevier, Amsterdam **2017**, p. 643.
[13] J. Sun, W. Wei, Y. Xu, J. Qu, X. Liu, T. Endo, *RSC Adv.* **2015**, *5*, 19048.
[14] P. Yang, X. Wang, H. Fan, Y. Gu, *PCCP* **2013**, *15*, 15333.
[15] W.-K. Kim, W. L. Mattice, *Langmuir* **1998**, *14*, 6588.
[16] J. Shi, X. Zheng, L. Xie, F. Cao, Y. Wu, W. Liu, *Eur. Polym. J.* **2013**, *49*, 4054.
[17] P. Lorjai, S. Wongkasemjit, T. Chaisuwan, A. M. Jamieson, *Polym. Degrad. Stab.* **2011**, *96*, 708.
[18] S. Mahadik-Khanolkar, S. Donthula, A. Bang, C. Wisner, C. Sotiriou-Leventis, N. Leventis, *Chem. Mater.* **2014**, *26*, 1318.
[19] S. Taskin Omer, B. Kiskan, A. Aksu, N. Balkis, J. Weber, Y. Yagci, *Chem. Eur. J.* **2014**, *20*, 10953.
[20] Y. Ertas, T. Uyar, *Polymer* **2016**, *84*, 72.
[21] Y. Ertas, T. Uyar, *Polymer* **2014**, *55*, 556.
[22] Y. Ertas, T. Uyar, *Carbohydr. Polym.* **2017**, *177*, 378.
[23] P. M. Budd, B. S. Ghanem, S. Makhseed, N. B. McKeown, K. J. Msayib, C. E. Tattershall, *Chem. Commun.* **2004**, *0*, 230.
[24] P. M. Budd, K. J. Msayib, C. E. Tattershall, B. S. Ghanem, K. J. Reynolds, N. B. McKeown, D. Fritsch, *J. Membr. Sci.* **2005**, *251*, 263.
[25] P. M. Budd, N. B. McKeown, D. Fritsch, *J. Mater. Chem.* **2005**, *15*, 1977.
[26] L. M. Robeson, *J. Membr. Sci.* **2008**, *320*, 390.
[27] P. M. Budd, N. B. McKeown, *Polym. Chem.* **2010**, *1*, 63.
[28] S. Makhseed, F. Ibrahim, J. Samuel, *Polymer* **2012**, *53*, 2964.
[29] H. J. Mackintosh, P. M. Budd, N. B. McKeown, *J. Mater. Chem.* **2008**, *18*, 573.
[30] J. S. Bonso, G. D. Kalaw, J. P. Ferraris, *J. Mater. Chem. A* **2014**, *2*, 418.
[31] C. Zhang, P. Li, B. Cao, *Ind. Eng. Chem. Res.* **2015**, *54*, 8772.
[32] C. Zhang, P. Li, B. Cao, *J. Appl. Polym. Sci.* **2016**, *133*, n/a.
[33] B. Satilmis, T. Uyar, *J. Colloid Interface Sci.* **2018**, *516*, 317.
[34] B. Satilmis, P. M. Budd, *RSC Adv.* **2014**, *4*, 52189.
[35] B. Satilmis, P. M. Budd, T. Uyar, *React. Funct. Polym.* **2017**, *121*, 67.
[36] B. Satilmis, T. Uyar, *ACS Appl. Nano Mater.* **2018**, *1*, 1631.
[37] H. Yin, Y. Z. Chua, B. Yang, C. Schick, W. J. Harrison, P. M. Budd, M. Böhning, A. Schönhals, *J. Phys. Chem. Lett.* **2018**, *9*, 2003.

